Volume 53
Number 32
28 August 2024
Pages 13219-13680

Dalton Transactions

An international journal of inorganic chemistry

rsc.li/dalton

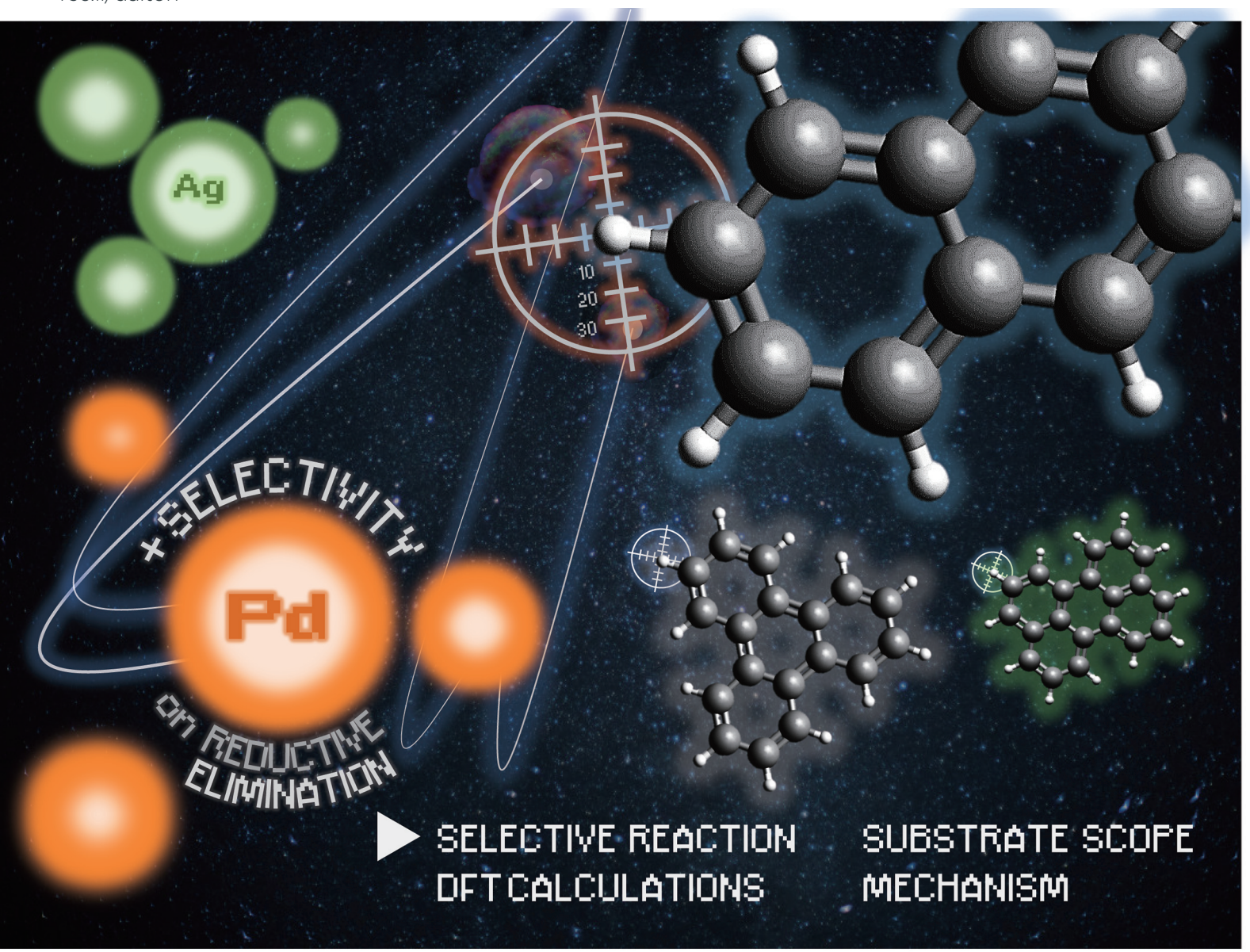

ISSN 1477-9226

ROYAL SOCIETY OF CHEMISTRY

PAPER

Takaki Kanbara, Junpei Kuwabara *et al.*
Mechanistic study on the reductive elimination of (aryl)(fluoroaryl)palladium complexes: a key step in regiospecific dehydrogenative cross-coupling

Dalton Transactions

ROYAL SOCIETY OF CHEMISTRY

PAPER

View Article Online
View Journal | View Issue

Cite this: *Dalton Trans.*, 2024, **53**, 13340

Mechanistic study on the reductive elimination of (aryl)(fluoroaryl)palladium complexes: a key step in regiospecific dehydrogenative cross-coupling†

Tomoki Iida,[a] Ryota Sato,[a] Yusuke Yoshigoe,[b] Takaki Kanbara *[a] and Junpei Kuwabara *[a,c]

Cross-dehydrogenative coupling (CDC) reactions have attracted attention as short-step synthetic methods for C–C bond formation. Recently, we have developed CDC reactions between naphthalene and fluorobenzene. Rather than exhibiting general regioselectivity, this reaction proceeds selectively at the β-position of naphthalene. In this study, investigation using model complexes as reaction intermediates revealed that the origin of the unique selectivity is the exclusive occurrence of reductive elimination at the β-position. Detailed studies on the reductive elimination showed that the steric hindrance of the naphthyl group and the electron-withdrawing properties of fluorobenzene determine the position at which the reductive elimination reaction proceeds. These results show that the selectivity of the C–H functionalisation of polycyclic aromatic hydrocarbons (PAHs) is determined not by the C–H cleavage step, but by the subsequent reductive elimination step. The regioselective CDC reaction was adaptable to various PAHs but was less selective for pyrene with extended π-conjugation. In fluorobenzene substrates, the F atoms at the two *ortho* positions of the C–H moiety are necessary for high selectivity. The substrate ranges are in good agreement with the proposed mechanism, in which the reductive elimination step determines the regioselectivity.

Received 17th May 2024,
Accepted 28th June 2024

DOI: 10.1039/d4dt01453g

rsc.li/dalton

Introduction

Cross-coupling reactions are important bond-forming reactions that facilitate the syntheses of various natural products, pharmaceuticals, and electronic device materials.[1,2] Conventional cross-coupling reactions entail the preparation of organometallic reagents, such as organoboron or organotin compounds, and halogenated compounds. In contrast, cross-dehydrogenative coupling (CDC) reactions, which enable cross-coupling between C–H bonds, have attracted attention as short-step synthetic methods that do not require pre-functionalisation.[3–12] CDC reactions between electron-rich thiophenes and electron-deficient fluorobenzenes have been demonstrated to exhibit high cross-coupling selectivity and regioselectivity, without requiring a directing group.[13–16] Recently, we extended this strategy and realized a selective cross-coupling CDC reaction of fluorobenzenes with less-reactive naphthalenes through the cooperative effect of a Pd catalyst and Ag salt.[17] Interestingly, this reaction preferentially proceeds at the β-position of naphthalene although the C–H direct functionalisation of naphthalene preferentially occurs at the α-position in general.[18–20] The investigation into the origin of this unique selectivity indicated that the formation of the α-substituted product is suppressed owing to the very slow reductive elimination of a Pd(II) complex with an α-naphthyl group (α-biaryl complex; Scheme 1b).[17]

In addition to the reversibility of the C–H cleavage of naphthalene, the β-substituted product is preferentially formed from the β-biaryl complex owing to rapid reductive elimination (Scheme S1†). The reaction mechanism is noteworthy because the regioselectivity of direct C–H functionalisation is determined by the reductive elimination step rather than by the C–H cleavage step. As reductive elimination is a critical elemental reaction that yields products in many cross-coupling reactions,[21–24] the detailed studies have been conducted in Ni,[25] Pd,[26,27] and Pt[28,29] complexes. However, it rarely determines the regioselectivity of general C(sp^2)–C(sp^2) coupling reactions owing to its rapid nature. In special cases in silaboration and C–N coupling reactions, reductive elimination has been reported to determine regioselectivity.[30,31] The

[a]*Institute of Pure and Applied Sciences, University of Tsukuba 1-1-1 Tennodai, Tsukuba, Ibaraki 305-8573, Japan. E-mail: kanbara@ims.tsukuba.ac.jp*
[b]*Department of Chemistry, Faculty of Science, Tokyo University of Science, 1-3 Kagurazaka, Shinjuku, Tokyo 162-8601, Japan*
[c]*Tsukuba Research Center for Energy Materials Science (TREMS), Institute of Pure and Applied Sciences, University of Tsukuba 1-1-1 Tennodai, Tsukuba, Ibaraki 305-8573, Japan. E-mail: kuwabara@ims.tsukuba.ac.jp*

†Electronic supplementary information (ESI) available. CCDC 2338608 and 2338609. For ESI and crystallographic data in CIF or other electronic format see DOI: https://doi.org/10.1039/d4dt01453g

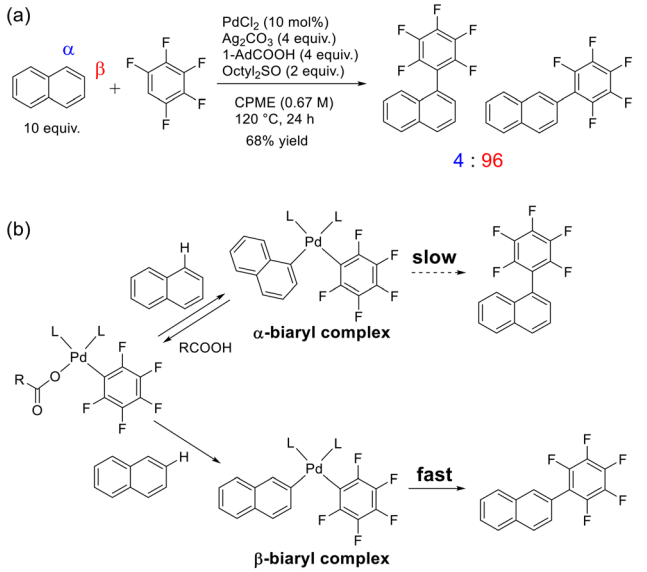

Scheme 1 (a) β-Selective CDC reaction; (b) proposed reaction mechanism for β-selectivity.[17]

aim of this study is to uncover the origin of the rate difference in reductive elimination, which determines regioselectivity. The findings demonstrate that the difference in the reductive elimination rates was caused by the steric hindrance of naphthalene and the electron-withdrawing effect of fluorobenzenes. Moreover, this mechanism provides a plausible explanation for the substrate scope of the regioselective CDC reaction. This study offers essential insights into the CDC and reductive elimination which is a crucial elementary reaction in organometallic chemistry.

Results and discussion

Rate differences in reductive elimination

Previously, the biaryl model complexes with *N*,*N*,*N*′,*N*′-tetramethylethylenediamine (TMEDA) as a supporting ligand were synthesised and compared in terms of reductive elimination (Scheme 2).[17] Reductive elimination of the α-biaryl model complex did not proceed at 120 °C in cyclopentyl methyl ether (CPME) under the same conditions used for the catalytic reaction. One factor that prevents reductive elimination even at such high temperatures is the effect of the electron-withdrawing pentafluorophenyl group.[16,32–37] In contrast, the β-biaryl model complex reacted entirely in 10 min, yielding the reductive elimination product (92%), as well as naphthalene (7%) as a decomposed product.[17] These results show that the reductive elimination of the β-biaryl model complex is significantly faster than that of the α-biaryl model complex. To understand the reason for the difference in the reductive elimination rates, these two complexes were analyzed using single-crystal X-ray structural analysis (Fig. S1†). The Pd–C distances between Pd and C_6F_5 in the two complexes were almost the same. The

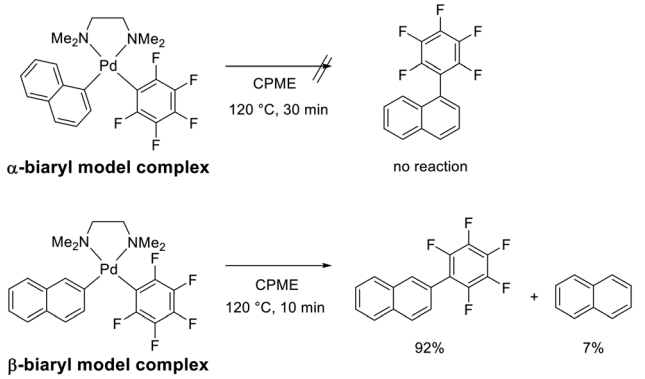

Scheme 2 Differences in reactivity of reductive elimination in the model complexes.[17]

naphthalene moiety was disordered; hence, no clear comparison could be made for the distance between Pd and the naphthalene carbon. Comparing ^{19}F nuclear magnetic resonance (NMR) spectra, five signals were observed in the α-biaryl model complex, whereas only three signals were observed in the β-biaryl model complex (Fig. S3 and S5†), which indicates that the rotation of the C_6F_5 group in the α-biaryl model complex is slower than the NMR timescale. The five signals of the α-biaryl model complex did not coalesce even at 110 °C. These results suggest that the rotation of the aryl group is inhibited in the α-biaryl model complexes, presumably due to a steric requirement. This sterically restricted structure may be associated with slow reductive elimination.[38–40] When 1-adamantanecarboxylic acid was added to the α-biaryl model complex and heated, naphthalene was formed by the reverse reaction (Scheme 1b, and Scheme S2†). In addition, the β-substituted coupling product, 2-(pentafluorophenyl) naphthalene, was observed in small amounts (Scheme S3†). The formation of the β-substituted coupling product from the α-biaryl model complex shows the reverse reaction and cleavage of the C–H bond at the β-position, followed by reductive elimination (see Scheme 1b).

The reductive elimination of the β-biaryl model complex was found to be faster than that of the α-biaryl model complex. However, as the steric and electronic factors are different at the α- and β-positions of the naphthyl group, the factor responsible for the difference in the reductive elimination rate is not clear. To compare only the steric factors under almost the same electronic factors, complexes with *ortho*-tolyl and *para*-tolyl groups were investigated instead of the α-naphthyl and β-naphthyl groups (Scheme 3). In CPME at 120 °C, the complex with the *ortho*-tolyl group, which has a large steric hindrance, showed no reaction at all, whereas the complex with the *para*-tolyl group showed quantitative reductive elimination (Fig. S6†). This indicates that steric hindrance was the principal factor in decreasing the rate of reductive elimination. Although the steric hindrance of phosphorus ligands is known to promote reductive elimination by destabilizing biaryl intermediates,[23,41–43] the effect of the steric hindrance of the aryl group on the reductive elimination between sp^2 carbons

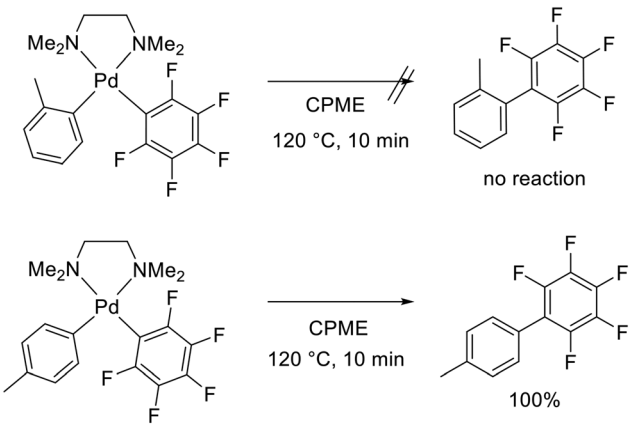

Scheme 3 Reductive elimination of *ortho*-tolyl and *para*-tolyl complex.

from Pd has not been discussed in detail. In reductive elimination for C–S and C–P bond formation, the steric hindrance of the aryl group on Pd reduces the rate.[44,45] Furthermore, the fact that Pd(2,4,6-trimethylphenyl)$_2$(tmeda) is stable at high temperature[40] also suggests that the steric hindrance of the aryl group inhibits reductive elimination. In Ir complexes, steric hindrance has been shown to slow reductive elimination.[46]

As mentioned above, no reductive elimination proceeded in the α-biaryl model complex at 120 °C for 30 min; however, when PPh_3 was added to the reaction system, complete reductive elimination proceeded in 30 min (Scheme 4, and Fig. S7†). As PPh_3 is more effective than TMEDA in promoting reductive elimination due to its π-acceptor nature,[47–50] reductive elimination proceeds at the α-position. The substitution of the chelating ligand TMEDA with PPh_3 may have facilitated the formation of a three-coordinate state and accelerated reductive elimination.[24] The choice of supporting ligands that did not promote reductive elimination, such as TMEDA used in this model system and the dialkyl sulfoxide additive used in the coupling reaction, was identified as a contributing factor to the observed differences in reductive elimination.

Kinetic parameters in reductive elimination of β-biaryl model complexes

As the β-biaryl model complex can be isolated and undergoes selective reductive elimination, detailed studies of this process are feasible. The kinetic parameters of the reductive elimination were calculated by tracing the reaction over time.[51,52] Heating of the β-biaryl model complex in deuterated toluene revealed that reductive elimination proceeds in accordance with the first-order reaction kinetic equation (Fig. 1a). The rate constants at each temperature were used to calculate the activation enthalpy ($\Delta H^{\ddagger}$) and entropy ($\Delta S^{\ddagger}$), as a linear relationship was obtained from an Eyring plot. The results yielded $\Delta H^{\ddagger}$ = 134 kJ mol^{-1}, $\Delta S^{\ddagger}$ = 73 J K^{-1} mol^{-1} (Fig. 1b). As the Eyring plot is not a perfect straight line, these values may contain a certain amount of error. In particular, large differences in $\Delta S^{\ddagger}$ values can be observed for small differences in slope. Osakada *et al.* have reported values of $\Delta H^{\ddagger}$ = 101 kJ mol^{-1} and $\Delta S^{\ddagger}$ = −10 J K^{-1} mol^{-1} in the reductive elimination of a similar complex (Fig. 2) in deuterated benzene.[51] The high $\Delta H^{\ddagger}$ of the β-biaryl model complex is presumably due to the large number of F substituents. However, the reason for the

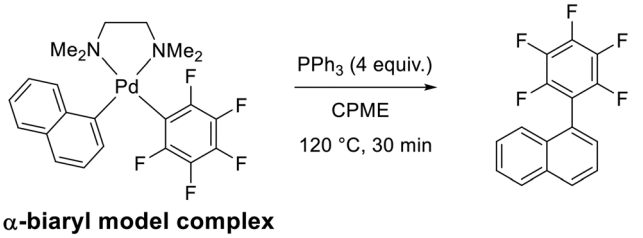

Scheme 4 Reductive elimination of α-biaryl model complex with PPh_3.

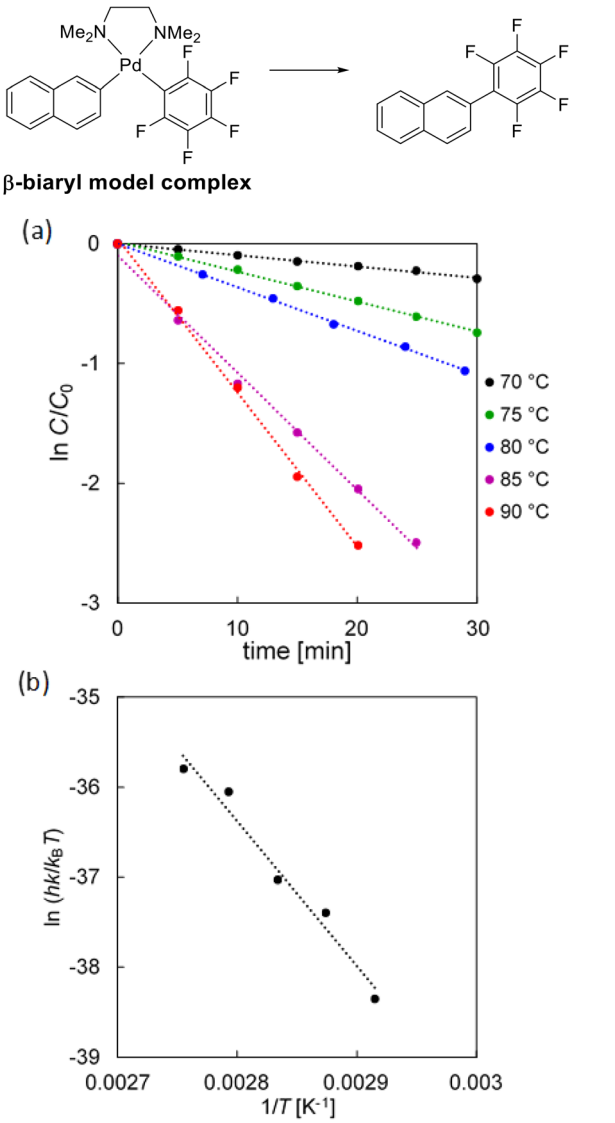

Fig. 1 (a) First-order plot of reductive elimination of the β-biaryl model complex in toluene-d_8, (b) Eyring plot.

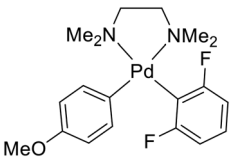

Fig. 2 Reported complex for comparison.[51]

positive value of $\Delta S^{\ddagger}$ in the β-biaryl model complex is unclear. This may be due to the elongation of the Pd–C bond in the transition state, which enables greater degrees of freedom.

The kinetic parameters were calculated for several deuterated solvents to investigate their effects on reductive elimination. Similar values were obtained for the low-polarity solvents deuterated toluene, dioxane, and tetrachloroethane (Table 1). In the high-polarity solvents, CD_3NO_2 and DMSO-d_6, the values of $\Delta H^{\ddagger}$ became smaller, and the values of $\Delta S^{\ddagger}$ were close to zero. Particularly in DMSO-d_6, the value of $\Delta S^{\ddagger}$ was negative. A possible reason for this negative value is that the DMSO molecule is directly involved in the transition state, resulting in multimolecular reactions. However, when the coordination of other molecules is involved in the transition state of reductive elimination, the value of $\Delta S^{\ddagger}$ is more negatively significant. For example, in a reaction in which reductive elimination is promoted by the coordination of an olefin to the apical position of a Ni(II) diethyl complex, the value of $\Delta S^{\ddagger}$ is −53.5 J K^{-1} mol^{-1}.[25] Therefore, we assume that DMSO is not directly involved in the transition state. As the values of $\Delta H^{\ddagger}$ are small in high-polarity solvents, CD_3NO_2 and DMSO-d_6, high-polarity solvents may facilitate the formation of structures such as tricoordinate intermediates, which favour reductive elimination.[50] Table 1 displays the $\Delta G^{\ddagger}$ values at 120 °C, at which the CDC reaction occurs. The $\Delta G^{\ddagger}$ values indicate that reductive elimination proceeds more easily in low-polarity solvents at a high temperature of 120 °C.

Table 1 Kinetic parameters of the reductive elimination reactions of the β-biaryl model complex and dielectric constants of solvents[53]

Solvent	Dielectric constants	$\Delta H^{\ddagger}$ (kJ mol^{-1})	$\Delta S^{\ddagger}$ (J K^{-1} mol^{-1})	$\Delta G^{\ddagger}$ (kJ mol^{-1}; 120 °C)
Toluene-d_8	2.38	134	73	105
Dioxane-d_8	2.21	131	56	109
$C_2D_2Cl_4$	8.2	141	91	105
CD_3NO_2	35.8	119	16	113
DMSO-d_6	42	104	−15	110

Discussion based on theoretical calculations

For a detailed understanding of the difference in the transitional barrier of reductive elimination between the α- and β-biaryl model complexes, these reactions were modeled using theoretical calculations at the B3LYP/6-311+G(d,p) (with SDD for Pd) level in CPME (ε = 4.76) solution (Fig. 3). Each reductive elimination process for both complexes begins with a carbon

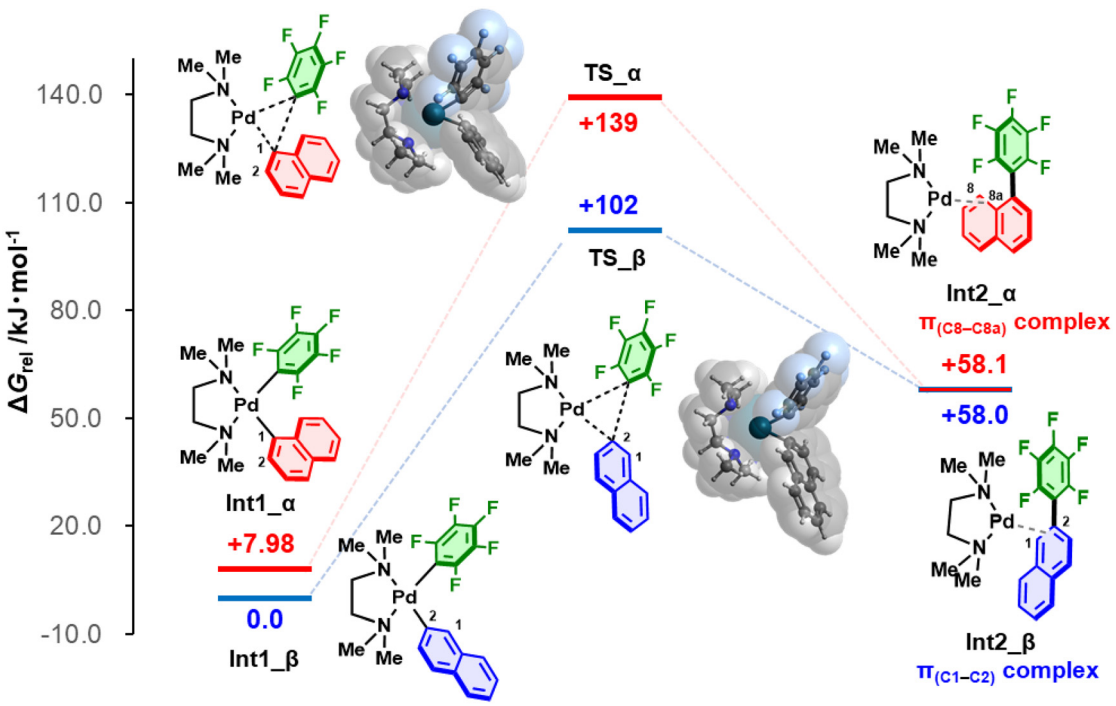

Fig. 3 Free-energy profiles of the modeled reaction pathways for the reductive elimination of the α- and β-biaryl model complexes at the B3LYP/6-311+G(d,p) (with SDD for Pd) level in CPME (ε = 4.76) solution. All ΔG_{rel} values represent the relative Gibbs energy for the complex compared to the Gibbs energy for **Int1-β**. (ΔG_{rel} = (*G* of any complex) − (*G* of **Int1-β**). Transition energies, $\Delta G^{\ddagger}$ = ΔG_{rel} (TS) − ΔG_{rel} (**int1**), were calculated to be 131 and 102 kJ mol^{-1} for the α- and β-biaryl model complexes, respectively.

atom approaching another to create a C–C bond, followed by the formation of the π-coordination complex. Activation energy values, $\Delta G^{\ddagger}$, of these processes of the α- and β-biaryl model complexes were estimated to be 131 and 102 kJ mol^{-1}, respectively. The value for the β-biaryl model complex was comparable to the experimental value (*vide supra*). The value for the α-complex is considerably higher ($\Delta\Delta G^{\ddagger}$ = 29 kJ mol^{-1}) than that for the β-complex. In the transition state of the α-biaryl model complex, the pentafluorophenyl and naphthyl rings are arranged with a twisted torsion of 25.6° due to the proximity of the H and F atoms on the rings. Conversely, the β-biaryl model complex exhibits less torsion, at 0.7°. Reduced torsion enables the overlap of orbitals between two carbon atoms, facilitating the reductive elimination of the β-biaryl model complex.

Substrate scope of the regioselective CDC reaction

The substrate scope of the regioselective CDC reaction was investigated using polycyclic aromatic hydrocarbons (PAHs). In addition to the previously reported naphthalene and anthracene,[17,54] phenanthrene, perylene, triphenylene, and pyrene were examined as typical examples of common PAHs (Scheme 5).[55–62] Because the aim was to investigate the correlation between regioselectivity and the structure of the substrates, the reaction conditions were not optimized for each substrate, and all reactions were performed under identical conditions. The CDC reaction of phenanthrene with pentafluorobenzene afforded a mixture of two isomers, 2- and 3-pentafluorophenyl phenanthrene. The positions of the introduced pentafluorophenyl groups were determined by comparison with the NMR spectra of separately synthesised reference compounds (Fig. S23†). Although C–H functionalisation of phenanthrene typically occurs at position 9,[63–67] this reaction does not produce the 9-substituted product. This observation shows that selectivity is determined by the steric demand for phenanthrene. Pentafluorobenzene was introduced at position 2 of triphenylene (Fig. S34†). The yield and selectivity of perylene were calculated from the NMR spectra of the reaction mixture, because isolating the product from the remaining perylene was difficult. The results showed that the reaction proceeds selectively at the sterically vacant position 2 of perylene (Fig. S37†). In contrast, pyrene yielded products that reacted at positions 1 and 4, in addition to the sterically vacant position 2 (Fig. S42†). This result shows that reductive elimination proceeds even at the sterically hindered positions 1 and 4 in pyrene.

Reductive elimination is more likely when the aryl group is electron-rich.[52] As pyrene has a more extended π-conjugation than the other substrates examined in this study, abundant π-electrons might facilitate reductive elimination, resulting in low regioselectivity. Theoretical calculations were performed to determine the activation energy value $\Delta G^{\ddagger}$ of the reductive elimination of Pd(pyrenyl)C_6F_5(tmeda) with pyrene bound to Pd in the 1- or 2-position. These calculations were carried out in a similar manner to those performed for the α- and β-biaryl model complexes bearing the naphthyl moiety. The ΔG of reductive elimination of Pd(2-pyrenyl)C_6F_5(tmeda), which is less sterically hindered, is lower than that of Pd(1-pyrenyl)C_6F_5(tmeda). This is the same trend as for naphthalene. However, the $\Delta\Delta G$ between the 2-pyrenyl and 1-pyrenyl complexes is only 7 kJ mol^{-1}, which is significantly less than the

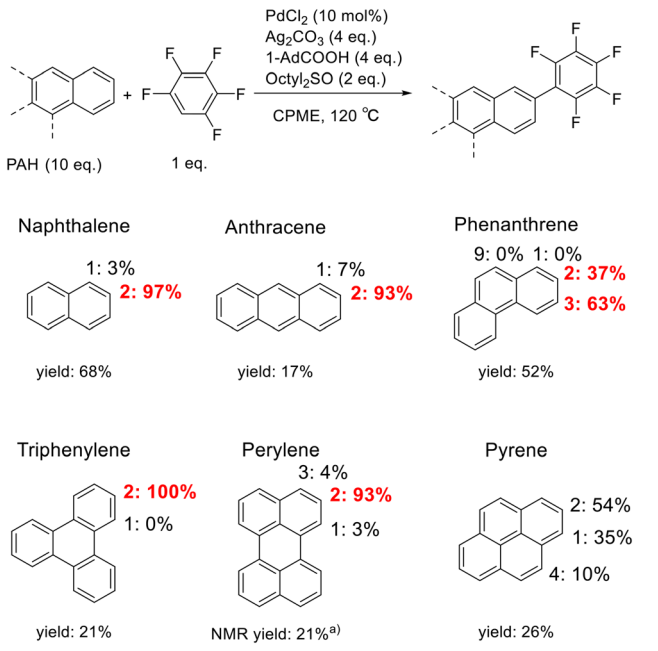

Scheme 5 CDC reaction of pentafluorobenzene with various PAHs. (a) NMR yield and regioselectivity were determined *via* ^{19}F NMR analysis of a crude product with hexafluorobenzene as an internal standard.

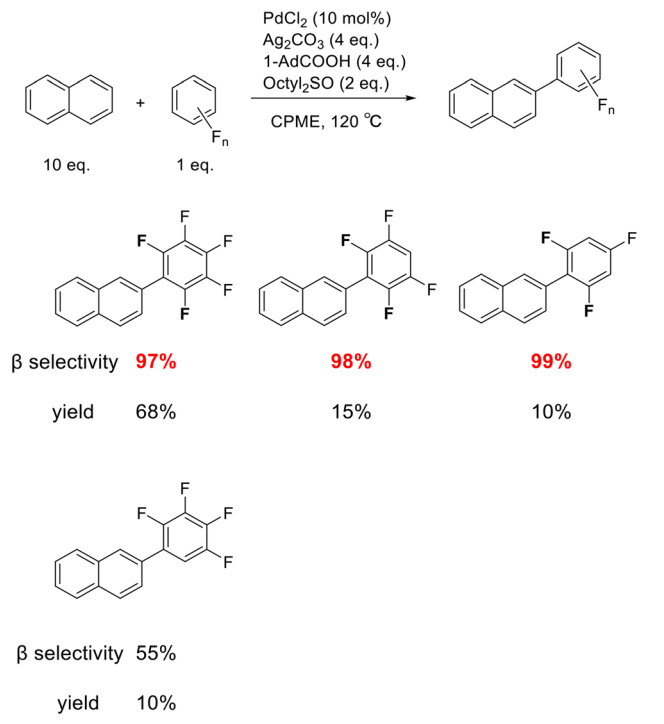

Scheme 6 CDC reaction of naphthalene with various fluorobenzenes.

29 kJ mol^{-1} between the α and β-biaryl model complexes bearing a naphthyl moiety. These results support that the small difference in the rate of reductive elimination in the case of pyrene is a factor in the low selectivity of the CDC reaction. In terms of substrate scope of PAHs, regiospecific reactions occur in many PAHs; however, the selectivity is low in π-electron-rich substrates.

The scope of the fluorobenzene substrates was also investigated. In addition to previously reported pentafluorobenzenes, high selectivities were observed for 1,2,4,5-tetrafluorobenzene and 1,3,5-trifluorobenzene (Scheme 6). In contrast, the reaction with 1,2,3,4-tetrafluorobenzene resulted in a low β-selectivity of 55%. These results indicated that the introduction of F at both *ortho*-positions of the C–H bond was essential for achieving high regioselectivity. The F atoms at the two *ortho*-positions of the aryl group on Pd have been reported to undergo slow reductive elimination.[51,68] This suggests that the two F atoms at the *ortho*-positions limit the reductive elimination, thereby exhibiting regioselectivity.

Conclusion

This study elucidates the origin of the unique regioselectivity of the CDC reaction between fluorobenzenes and PAHs, which proceeds predominantly in sterically vacant positions. Investigation of the reactivity of the reaction intermediates revealed that the unique regioselectivity was determined by the reductive elimination step rather than the C–H cleavage step. Specifically, the steric hindrance of PAHs and the electron-withdrawing effect of the pentafluorophenyl group limit the positions at which the reductive elimination reaction can proceed, resulting in a unique regioselectivity. Therefore, it is important to select ligands that do not promote reductive elimination to achieve regioselectivity. The present regioselective CDC reaction can be adapted to a variety of PAHs; however, it was less selective in π-electron-rich pyrene. For fluorobenzenes, substrates with F atoms introduced at the two *ortho*-positions of the C–H bond demonstrated high selectivity. These substrate scopes are consistent with the mechanism uncovered in the present study, in which regioselectivity is determined by the reductive elimination step. While studying the reductive elimination of Pd biaryl complexes with various aryl and pentafluorophenyl groups ($PdArC_6F_5$(tmeda)), it was established that complexes with large steric hindrance of the eliminating aryl group underwent slow reductive elimination. These results suggest that the coupling of sterically hindered aromatic compounds with fluorobenzenes is difficult because of reductive elimination. These findings provide fundamental insights into organometallic and synthetic organic chemistry.

Data availability

All experimental data is available in the ESI.†

• The data supporting this article have been included as part of the ESI.†

• Crystallographic data for α-biaryl model complex and β-biaryl model complex has been deposited at the CCDC under 2338608 and 2338609,† and can be obtained from **https://www.ccdc.cam.ac.uk/**.

Author contributions

T. Iida performed experiments, analyzing data, and wrote the manuscript with support from J. Kuwabara. R. Sato performed experiments, analyzing data. Y. Yoshigoe provided a discussion based on DFT calculations. T. Kanbara has advised the project from an organometallic chemistry perspective. J. Kuwabara is involved in project development, supervision, and submission. All authors have read and agreed to the published version of the manuscript.

Conflicts of interest

There are no conflicts to declare.

Acknowledgements

The authors thank the Chemical Analysis Center of the University of Tsukuba for the measurements of NMR, and the single-crystal X-ray diffraction. This work was partially supported by JST A-STEP Grant Number JPMJTM22AR and JSPS KAKENHI Grant Number 22K05075.

References

1 *Applied Cross-Coupling Reactions*, ed. Y. Nishihara, Springer Berlin Heidelberg, Berlin, Heidelberg, 2013, vol. 80.
2 H. Li, C. C. C. Johansson Seechurn and T. J. Colacot, *ACS Catal.*, 2012, **2**, 1147–1164.
3 D. R. Stuart and K. Fagnou, *Science*, 2007, **316**, 1172–1175.
4 Y. Yang, J. Lan and J. You, *Chem. Rev.*, 2017, **117**, 8787–8863.
5 Y. F. Zhang and Z. J. Shi, *Acc. Chem. Res.*, 2019, **52**, 161–169.
6 B. Chakraborty and C. K. Luscombe, *Angew. Chem., Int. Ed.*, 2023, **62**, e202301247.
7 Y. Yang, Y. Wu, Z. Bin, C. Zhang, G. Tan and J. You, *J. Am. Chem. Soc.*, 2024, **146**, 1224–1243.
8 G. Albano, *Org. Chem. Front.*, 2024, **11**, 1495–1622.
9 Y. Wei and W. Su, *J. Am. Chem. Soc.*, 2010, **132**, 16377–16379.
10 C. Sambiagio, D. Schönbauer, R. Blieck, T. Dao-Huy, G. Pototschnig, P. Schaaf, T. Wiesinger, M. F. Zia, J. Wencel-Delord, T. Besset, B. U. W. Maes and M. Schnürch, *Chem. Soc. Rev.*, 2018, **47**, 6603–6743.

11 K. L. Hull and M. S. Sanford, *J. Am. Chem. Soc.*, 2007, **129**, 11904–11905.
12 H. Li, J. Liu, C. L. Sun, B. J. Li and Z. J. Shi, *Org. Lett.*, 2011, **13**, 276–279.
13 C. Y. He, S. Fan and X. Zhang, *J. Am. Chem. Soc.*, 2010, **132**, 12850–12852.
14 C. Y. He, Q. Q. Min and X. Zhang, *Organometallics*, 2012, **31**, 1335–1340.
15 H. Aoki, H. Saito, Y. Shimoyama, J. Kuwabara, T. Yasuda and T. Kanbara, *ACS Macro Lett.*, 2018, **7**, 90–94.
16 Y. Shimoyama, J. Kuwabara and T. Kanbara, *ACS Catal.*, 2020, **10**, 3390–3397.
17 R. Sato, T. Iida, T. Kanbara and J. Kuwabara, *Chem. Commun.*, 2022, **58**, 11511–11514.
18 R. Li, L. Jiang and W. Lu, *Organometallics*, 2006, **25**, 5973–5975.
19 A. Petit, J. Flygare, A. T. Miller, G. Winkel and D. H. Ess, *Org. Lett.*, 2012, **14**, 3680–3683.
20 D. Kim, G. Choi, W. Kim, D. Kim, Y. K. Kang and S. H. Hong, *Chem. Sci.*, 2021, **12**, 363–373.
21 J. M. Brown and N. A. Cooley, *Chem. Rev.*, 1988, **88**, 1031–1046.
22 A. Yamamoto, T. Yamamoto and F. Ozawa, *Pure Appl. Chem.*, 1985, **57**, 1799–1808.
23 J. F. Hartwig, *Inorg. Chem.*, 2007, **46**, 1936–1947.
24 K. Tatsumi, R. Hoffmann, A. Yamamoto and J. K. Stille, *Bull. Chem. Soc. Jpn.*, 1981, **54**, 1857–1867.
25 T. Yamamoto, A. Yamamoto and S. Ikeda, *J. Am. Chem. Soc.*, 1971, **93**, 3350–3359.
26 A. Moravskiy and J. K. Stille, *J. Am. Chem. Soc.*, 1981, **103**, 4182–4186.
27 E. Negishi, T. Takahashi and K. Akiyoshi, *J. Organomet. Chem.*, 1987, **334**, 181–194.
28 P. S. Braterman, R. J. Cross and G. B. Young, *J. Chem. Soc., Dalton Trans.*, 1977, 1892–1897.
29 R. K. Merwin, R. C. Schnabel, J. D. Koola and D. M. Roddick, *Organometallics*, 1992, **11**, 2972–2978.
30 T. Ohmura, K. Oshima, H. Taniguchi and M. Suginome, *J. Am. Chem. Soc.*, 2010, **132**, 12194–12196.
31 A. Vogt, F. Stümpges, J. Bajrami, D. Baumgarten, J. Millan, E. Mena-Osteritz and P. Bäuerle, *Chem. – Eur. J.*, 2023, **29**, e202301867.
32 R. Uson, J. Fornies, J. Gimeno, P. Espinet and R. Navarro, *J. Organomet. Chem.*, 1974, **81**, 115–122.
33 G. López, G. García, N. Cutillas and J. Ruiz, *J. Organomet. Chem.*, 1983, **241**, 269–273.
34 E. Gioria, J. del Pozo, J. M. Martínez-Ilarduya and P. Espinet, *Angew. Chem., Int. Ed.*, 2016, **55**, 13276–13280.
35 Y. P. Budiman, A. Jayaraman, A. Friedrich, F. Kerner, U. Radius and T. B. Marder, *J. Am. Chem. Soc.*, 2020, **142**, 6036–6050.
36 J. Ponce-de-León, G. Marcos-Ayuso, J. A. Casares and P. Espinet, *Chem. Commun.*, 2022, **58**, 3146–3149.
37 R. Sato, T. Yasuda, T. Hiroto, T. Kanbara and J. Kuwabara, *Chem. – Eur. J.*, 2023, **29**, e202203816.
38 C. Bartolomé, P. Espinet, L. Vicente, F. Villafañe, J. P. H. Charmant and A. G. Orpen, *Organometallics*, 2002, **21**, 3536–3543.
39 C. Bartolomé, P. Espinet, J. M. Martín-Álvarez and F. Villafañe, *Eur. J. Inorg. Chem.*, 2004, **2004**, 2326–2337.
40 C. Bartolomé, F. Villafañe, J. M. Martín-Alvarez, J. M. Martínez-Ilarduya and P. Espinet, *Chem. – Eur. J.*, 2013, **19**, 3702–3709.
41 M. C. Nielsen, K. J. Bonney and F. Schoenebeck, *Angew. Chem., Int. Ed.*, 2014, **53**, 5903–5906.
42 T. E. Barder and S. L. Buchwald, *J. Am. Chem. Soc.*, 2007, **129**, 12003–12010.
43 R. Martin and S. L. Buchwald, *Acc. Chem. Res.*, 2008, **41**, 1461–1473.
44 G. Mann, D. Baranano, J. F. Hartwig, A. L. Rheingold and I. A. Guzei, *J. Am. Chem. Soc.*, 1998, **120**, 9205–9219.
45 R. A. Stockland, A. M. Levine, M. T. Giovine, I. A. Guzei and J. C. Cannistra, *Organometallics*, 2004, **23**, 647–656.
46 R. Ghosh, T. J. Emge, K. Krogh-Jespersen and A. S. Goldman, *J. Am. Chem. Soc.*, 2008, **130**, 11317–11327.
47 N. Fey, A. G. Orpen and J. N. Harvey, *Coord. Chem. Rev.*, 2009, **253**, 704–722.
48 M. J. Wovkulich, J. L. Atwood, L. Canada and J. D. Atwood, *Organometallics*, 1985, **4**, 867–871.
49 M. C. Kohler, T. V. Grimes, X. Wang, T. R. Cundari and R. A. Stockland, *Organometallics*, 2009, **28**, 1193–1201.
50 M. Pérez-Rodríguez, A. A. C. Braga, M. Garcia-Melchor, M. H. Pérez-Temprano, J. A. Casares, G. Ujaque, A. R. de Lera, R. Álvarez, F. Maseras and P. Espinet, *J. Am. Chem. Soc.*, 2009, **131**, 3650–3657.
51 K. Osakada, H. Onodera and Y. Nishihara, *Organometallics*, 2005, **24**, 190–192.
52 T. Korenaga, K. Abe, A. Ko, R. Maenishi and T. Sakai, *Organometallics*, 2010, **29**, 4025–4035.
53 A. A. Maryott and E. R. Smith, *Table of dielectric constants of pure liquids*, U. S. Govt. Print. Off, 1951, vol. 514.
54 R. Sato, K. Chen, T. Yasuda, T. Kanbara and J. Kuwabara, *Org. Chem. Front.*, 2023, **10**, 2955–2962.
55 S. Liu, L. Zheng, M. Chen, Y. Sun, P. Wang, S. Li, H. Wu, X. Zhang and W. Hu, *J. Mater. Chem. C*, 2021, **9**, 4217–4222.
56 S. Oda, K. Ueura, B. Kawakami and T. Hatakeyama, *Org. Lett.*, 2020, **22**, 700–704.
57 J. Merz, L. Dietrich, J. Nitsch, I. Krummenacher, H. Braunschweig, M. Moos, D. Mims, C. Lambert and T. B. Marder, *Chem. – Eur. J.*, 2020, **26**, 12050–12059.
58 L. Biesen, L. May, N. Nirmalananthan-Budau, K. Hoffmann, U. Resch-Genger and T. J. J. Müller, *Chem. – Eur. J.*, 2021, **27**, 13426–13434.
59 J. Wang, Y. Cui, S. Xie, J.-Q. Zhang, D. Hu, S. Shuai, C. Zhang and H. Ren, *Org. Lett.*, 2024, **26**, 137–141.
60 A. G. Crawford, Z. Liu, I. A. I. Mkhalid, M. H. Thibault, N. Schwarz, G. Alcaraz, A. Steffen, J. C. Collings, A. S. Batsanov, J. A. K. Howard and T. B. Marder, *Chem. – Eur. J.*, 2012, **18**, 5022–5035.

61 J. Wang, G. Meng, K. Xie, L. Li, H. Sun and Z. Huang, *ACS Catal.*, 2017, **7**, 7421–7430.
62 H. Fang, Q. He, G. Liu and Z. Huang, *Org. Lett.*, 2020, **22**, 9298–9302.
63 H. Kawai, Y. Kobayashi, S. Oi and Y. Inoue, *Chem. Commun.*, 2008, 1464–1466.
64 K. Funaki, H. Kawai, T. Sato and S. Oi, *Chem. Lett.*, 2011, **40**, 1050–1052.
65 K. Mochida, K. Kawasumi, Y. Segawa and K. Itami, *J. Am. Chem. Soc.*, 2011, **133**, 10716–10719.
66 K. D. Collins, R. Honeker, S. Vásquez-Céspedes, D. T. D. Tang and F. Glorius, *Chem. Sci.*, 2015, **6**, 1816–1824.
67 M. Shibata, H. Ito and K. Itami, *J. Am. Chem. Soc.*, 2018, **140**, 2196–2205.
68 Y. Nishihara, H. Onodera and K. Osakada, *Chem. Commun.*, 2004, 192–193.